Journal of Alloys and Compounds, 184 (1992) 35–42
JALCOM 163

Phase transformations in sputtered Nd–Fe–B alloys

Ya. L. Linetsky, V. M. Raigorodsky and V. Yu. Tsvetkov
The Laboratory of Magnetic Film Systems Technology, Moscow Institute of Steel and Alloys, Leninsky Prospect 4, 117936 Moscow (Russia)

(Received August 7, 1991; accepted in final form October 22, 1991)

Abstract

For sputtered $Nd_xFe_{93-x}B_7$ alloys (x = 9, 11, 13, 15, 16.5) a diagram of the intermediate stages when passing from the amorphous phase to stable crystalline phases is presented. The data were obtained at a heating rate of 20 K min^{-1} using X-ray diffraction and thermomagnetic and dilatometric methods. In understoichiometric alloys the transition from the amorphous phase to the crystalline phases α-Fe and $Nd_2Fe_{14}B$ proceeds through formation and decomposition of the metastable phases $Nd_2Fe_{16}B$ (type Nd_2Fe_{17}, T_c = 170 °C), $Nd_2Fe_{23}B_3$ (T_c = 380 °C) and ϵ (T_c = 250 °C). There first appears an α-Fe phase in the amorphous solid solution. In overstoichiometric alloys the transition to the structure consisting of $Nd_2Fe_{14}B$ and α-Nd phases proceeds through intermediate stages with metastable phases $Nd_2Fe_{23}B_3$ and χ (T_c = 170 °C). The first product of crystallization here is the χ phase.

1. Introduction

The method of target sputtering enables one to design multipole miniature magnetic systems as thin as 10^{-2}–10^2 μm [1]. The sputtering of alloys of rare earths with 3d metals on a metallic substrate at room temperature gives an amorphous structure which converts into a crystalline one on subsequent annealing. The transition from amorphous to crystalline structure is accompanied by significant intensification of the magnetic hysteresis. After deposition Nd–Fe–B-alloys have a coercivity $_IH_c$ = 10–10^2 Oe. Subsequent annealing at temperatures from 570 to 800 °C increases $_IH_c$ to 20 kOe for $Nd_{16.5}Fe_{76.5}B_7$ [2].

Amorphous alloys can also be obtained by melt spinning. Liao and Altounian [3] came to the conclusion that the crystallization near the $Nd_2Fe_{14}B$ composition of Nd–Fe–B amorphous alloys quenched from the liquid phase proceeds through only one exothermal stage, resulting in the formation of a stable phase structure. A similar result was also obtained in ref. 4, where the same alloys were investigated.

However, at equilibrium the compound $Nd_2Fe_{14}B$ is formed from the liquid phase by a peritectic reaction, *i.e.* the stoichiometric alloy crystallizes through several stages. In the metastable crystallization of cast alloys a phase of the type $Nd_2Fe_{17}B$ is involved [5]. This phase was also observed in the intermediate crystallization stage of amorphous sputtered Nd–Fe–Si–B alloys

0925-8388/92/$5.00

in ref. 6. Thus it may be supposed that in the case of sputtered Nd–Fe–B ternary alloys a transition to the stable crystalline phases will proceed through several intermediate stages realized within narrow temperature intervals. The goal of the present paper is to give an account of the discovery and investigation of these intermediate metastable stages.

2. Experimental details

Sputtered alloys were obtained by sputtering of the cast target $Nd_xFe_{93-x}B_7$ ($x=9$, 11, 13, 15, 16.5) at the rate of 40 μm h^{-1} on a water-cooled copper substrate. Films as thin as 250–300 μm were separated from the substrate and investigated in a vacuum dilatometer at a heating rate of 20 K min^{-1}. The Curie temperatures T_c of the ferromagnetic phases were measured by a vacuum magnetic microbalance in a maximal field of 100 Oe. X-ray diffraction measurements were performed on a DRON-3M diffractometer with Fe Kα radiation. Before examination the specimens were processed by electrolytic polishing. The intensities of the X-ray lines were calculated by the formula

$$I_{hkl}=f(\theta)|S_{hkl}|^2P_{hkl}\exp(-2M)$$

To compare the experimental and theoretical X-ray patterns, the following factor was applied:

$$R=\frac{\sum_{hkl}|I_{exp}-I_{theor}|}{\sum_{hkl}I_{exp}}$$

3. Experimental results and discussion

3.1. The alloy $Nd_{16.5}Fe_{76.5}B_7$

A dilatometric curve for $Nd_{16.5}Fe_{76.5}B_7$ is given in Fig. 1. The maximum temperature of the Invar-like part (section a) is close to the Curie temperature T_c of the amorphous phase. The temperature interval from 200 to 450 °C (section b) corresponds to normal thermal expansion of the amorphous phase with a mean linear expansion coefficient $\bar{\alpha}=14.5\times10^{-6}$ K^{-1}. There is a sharp peak (sections c and d) above 560 °C on the dilatometric curve.

Starting at 600 °C, $\bar{\alpha}$ continuously increases upon heating. The measured magnitude of $\bar{\alpha}$ of the amorphous alloy is close to the value of 16×10^{-6} K^{-1} reported previously for the massive polycrystalline alloy $Nd_2Fe_{14}B$ above T_c [7] and almost equal to the value of 14×10^{-6} K^{-1} derived from the cooling curve of the sputtered alloy in the interval 600–800 °C.

X-ray analysis of specimens with 16.5 at.% Nd quenched from the marked temperatures on the dilatometric curve of Fig. 1 reveals the presence of the amorphous phase at point 1, a mixture of amorphous and microcrystalline phases at point 2, an amorphous phase and the crystalline phases $Nd_2Fe_{14}B$

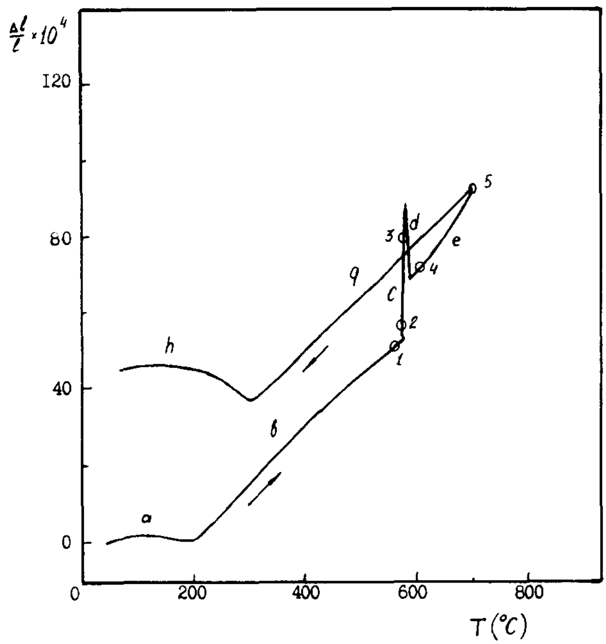

Fig. 1. Dilatometric curve of $Nd_{16.5}Fe_{76.5}B_7$.

(2:14:1), $Nd_2Fe_{23}B_3$ (2:23:3) and α-Nd (hexagonal) at point 3 and the phases 2:14:1 and α-Nd at points 4 and 5.

The results of thermomagnetic analysis of specimens quenched in the dilatometer from the different temperature points are given in Fig. 2. There is a peak in the differential thermomagnetic curve $dM(T)/dT$ (M, magnetization) of the specimen after sputtering. The corresponding Curie point is 220 °C. After quenching from point 1, T_c of the basic alloy component falls to 160 °C. At the same time there appears a small peak of a certain χ phase with $T_c=350$ °C. When the temperature is increased to point 2, apart from the two peaks mentioned above, there appears a strong peak from a phase with $T_c=305$ °C and also a small peak from a phase with $T_c=380$ °C. At point 3 the peak from the phase with $T_c=160$ °C disappears and only those of the phases with $T_c=305$, 350 and 380 °C remain. For specimens quenched from points 4 and 5 the differential thermomagnetic curves have quite similar shapes and possess only one peak from the phase with $T_c=305$ °C.

From the results of the present analysis the complex phase transformations occurring on heating the sputtered alloy $Nd_{16.5}Fe_{76.5}B_7$ can be represented in the following way. After sputtering, the films have an amorphous structure. On heating to 560 °C at a rate of 20 K min^{-1}, there occurs a phase, say χ, with $T_c=350$ °C. Simultaneously the amorphous phase composition changes and its T_c decreases from 220 to 160 °C. In the interval 560–570 °C the χ phase is present in microcrystalline form: it does not give clear reflections in the X-ray patterns. This phase is preserved also at higher temperatures up to 600 °C but in insufficient amounts to identify its crystal structure.

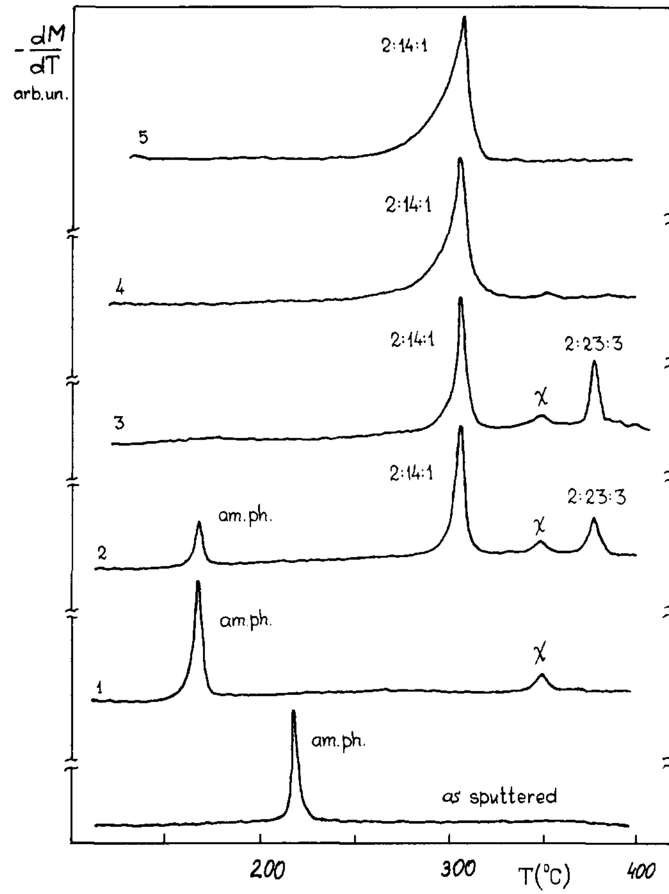

Fig. 2. Differential thermomagnetic curves of $Nd_{16.5}Fe_{76.5}B_7$ alloy specimens. The specimen numbers are identical to the point numbers (marking the heating temperatures of the specimens) on the dilatometric curve of Fig. 1.

Increasing the heating temperature to 570 °C (point 2) gives rise to a decrease in the amount of amorphous phase and results in the formation of the phases 2:14:1 (T_c=305 °C) and 2:23:3 (T_c=380 °C). Any small temperature variation (of about 5 °C) at the transition from point 2 to point 3 results in a strong expansion of the specimen apparently due to the appearance of pure neodymium in the structure, its density being noticeably smaller than that of the 2:14:1 and 2:23:3 phases. The subsequent compression seen in Fig. 1 reflects a transformation of the phase 2:23:3 and part of the neodymium into the 2:14:1 phase. The influence of the χ phase in the length variation is not too essential because of its small relative amount. In understoichiometric alloys (x=9, 11) neodymium is not formed and the peak marked by c–d in Fig. 1 is absent in the corresponding dilatometric curve (see Fig. 3).

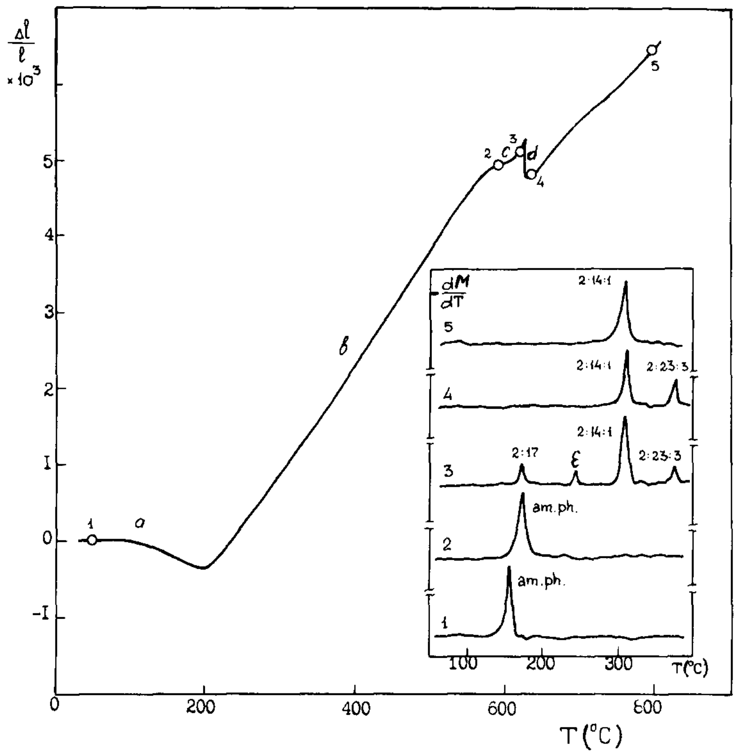

Fig. 3. Dilatometric heating curve of amorphous $Nd_{11}Fe_{82}B_7$ alloy. The thermomagnetic curves recorded after quenching of the specimens from the temperatures corresponding to the points marked on the dilatometric curve are given in the inset.

To summarize, the sequence of phase transformations observed when heating the sputtered alloy $Nd_{16.5}Fe_{76.5}B_7$ can be represented as follows:

$$\text{am.ph } (T_c = 220\ ^\circ\text{C}) \xrightarrow{560\ ^\circ\text{C}}$$
$$\text{am.ph } (T_c = 160\ ^\circ\text{C}) + \chi\ (T_c = 350\ ^\circ\text{C}) \xrightarrow{570\ ^\circ\text{C}}$$
$$\text{am.ph } (T_c = 160\ ^\circ\text{C}) + 2{:}14{:}1\ (T_c = 305\ ^\circ\text{C})$$
$$+ 2{:}23{:}3\ (T_c = 380\ ^\circ\text{C}) + \chi\ (T_c = 350\ ^\circ\text{C}) \xrightarrow{575\ ^\circ\text{C}}$$
$$2{:}14{:}1 + 2{:}23{:}3 + \alpha\text{-Nd} + \chi \xrightarrow{580\ ^\circ\text{C}} 2{:}14{:}1 + \alpha\text{-Nd}$$

3.2. *The alloy $Nd_{11}Fe_{82}B_7$*

In the understoichiometric alloys ($x = 9$, 11) the intermediate stages of the crystallization are realized over wider temperature intervals than in the overstoichiometric alloys.

On the dilatometric curve of the alloy with 11 at.% Nd there is an invar-type part (section a), a region of linear thermal expansion (section b), a region of length reduction (section c), a region of compression (section d) and a second region of linear thermal expansion.

Crystallization of this alloy starts at 570 °C by α-Fe formation. At 600 °C there appears a phase with the structure of the Th_2Zn_{17} type (2:17). The ratio of the atomic fractions of iron and neodymium in this phase was determined by minimizing the factor R calculated for the $NdFe_y$ phase (space group $R\bar{3}m$) with the lattice constants $a=0.8441$ nm and $c=1.2668$ nm. The values of R are equal to 18.8%, 13.5%, 8.9% and 10.5% for $y=7.0$, 7.5, 8.0 and 8.5 respectively. The Curie temperature of the 2:17 phase is 170 °C. The relatively high T_c of this phase as compared to the binary phase Nd_2Fe_{17} ($T_c=56$ °C) may be the result of the presence of B atoms in its structure. Taking into account the presence of small amounts of other boron compounds in the alloy after the thermal treatment near the lower bound of the temperature interval in which formation of the 2:17 phase can take place and guided by the minimum value of R for $y=8.0$, it is possible to express the phase composition as $Nd_2Fe_{16}B$. Note that in the metastable phase diagram of Nd–Fe–B reported in ref. 5 a phase Nd_2Fe_{17} near the composition $Nd_2Fe_{14}B$ is formed only in a narrow temperature interval (about 10 °C). Below this interval the 2:17 phase decomposes via the reaction $2{:}17+\mathrm{L}\rightarrow 2{:}14{:}1$. According to ref. 5, the composition of this phase can be expressed as $Nd_2Fe_{18}B$. During heating of sputtered alloys, formation of the 2:17 phase precedes formation of the 2:14:1 phase in the same way as during crystallization from the liquid state.

Apart from the 2:17 phase the phases α-Fe, 2:14:1 ($T_c=305$ °C), 2:23:3 ($T_c=380$ °C) and ϵ ($T_c=250$ °C) are also present in the alloy after heating to 600 °C. The volume fraction of the ϵ phase is insufficient to identify its crystal structure. The amounts of α-Fe, 2:14:1 and 2:23:3 increase during the heating process in region c, while the relative amount of the 2:17 phase decreases. After 1 h treatment at 600 °C the phase 2:23:3 has a b.c.c. structure with the lattice constant $a=1.412$ nm. The position and intensity of lines on its X-ray pattern inside the angle interval $2\theta=39°$–$115°$ correspond to those calculated under the assumption of space group $I\bar{4}3d$ and the structure basis proposed in ref. 8.

After thermal treatment at 630 °C and higher temperatures the alloy consists of 2:14:1 and α-Fe.

To summarize our results, phase transformations in the alloy $Nd_{11}Fe_{82}B_7$ during continuous heating at a rate of 20 °C min^{-1} proceed in the following sequence:

$$\text{am.ph } (T_c=155\ °C) \xrightarrow{570\ °C}$$

$$\text{am.ph } (T_c=175\ °C)+\alpha\text{-Fe} \xrightarrow{600\ °C}$$

$$2{:}17\ (T_c=170\ °C)+2{:}14{:}1\ (T_c=305\ °C)+\alpha\text{-Fe}$$

$$+2{:}23{:}3\ (T_c=380\ °C)+\epsilon\ (T_c=250\ °C) \xrightarrow{620\ °C}$$

$$2{:}14{:}1+\alpha\text{-Fe}+2{:}23{:}3+2{:}17 \xrightarrow{630\ °C} 2{:}14{:}1+\alpha\text{-Fe}$$

4. Conclusions

The results of the investigations of phase transformations in sputtered $Nd_xFe_{93-x}B_7$ alloys are represented in Fig. 4 in the form of intermediate stages. It has been shown that in both understoichiometric and overstoichiometric alloys the phase 2:14:1 is not a primary product of crystallization. The stoichiometric alloy has not been investigated in this paper. However, the appearance of the 2:23:3 phase in the understoichiometric and overstoichiometric alloys allows us to suppose that also in the stoichiometric alloy at least part of the basic 2:14:1 phase is formed as a result of reactions between crystalline phases formed earlier.

Five ferromagnetic crystalline phases have been observed in the understoichiometric alloys. Two of them are stable (α-Fe and 2:14:1) and three metastable (ϵ, 2:17 and 2:23:3).

Three ferromagnetic phases have been observed in the overstoichiometric alloys: a stable phase (2:14:1) and two metastable phases (2:23:3 and χ). The phase with $T_c = 250$ °C has been observed previously in the cast alloys Fe–80Nd–5B and Fe–40Nd–6.5B [9]. The χ phase with $T_c = 350$ °C has not been observed in Nd–Fe–B alloys before.

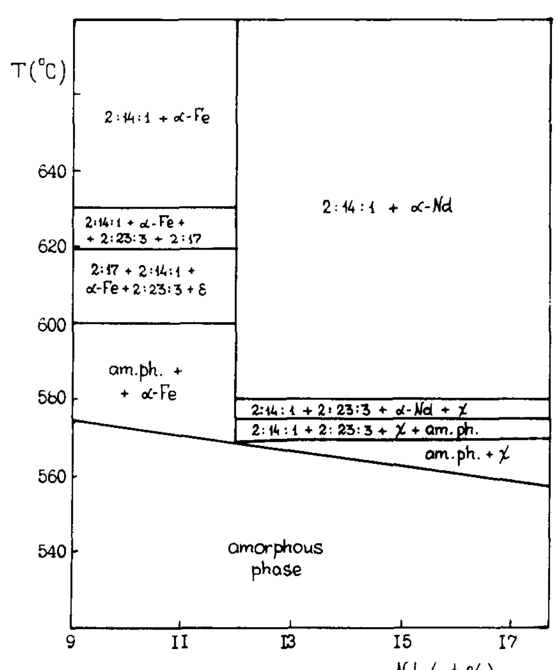

Fig. 4. Diagram of intermediate stages for $Nd_xFe_{93-x}B_7$ alloys (heating rate 20 K min^{-1}).

References

1 F. I. Cadieu, *J. Appl. Phys.*, *61* (1987) 4105.
2 B. S. Vekshin, B. A. Kapitanov, N. V. Kornilov, Ya. L. Linetsky, V. U. Raigorodsky, S. E. Sokolovsky and V. Yu. Tsvetkov, *Electrotechnika*, *11* (1989) 18.
3 L. X. Liao and Z. Altounian, *J. Appl. Phys.*, *66* (1989) 768.
4 K. H. J. Buschow, D. B. de Mooij and H. M. van Noort, *J. Less-Common Met.*, *125* (1986) 135.
5 B. Grieb, G. Schneider, E.-Th. Henig and G. Petzow, *Z. Metallk.*, *80* (1989) 515.
6 V. M. Raigorodsky, Ya. L. Linetsky, S. E. Sokolovsky and V. Yu. Tzvetkov, *Izv. VUZOV, Tchern. Metall.*, *9* (1990) 56.
7 K. H. J. Buschow, *J. Less-Common Met.*, *118* (1986) 349.
8 D. B. de Mooij and K. H. J. Buschow, *Philips J. Res.*, *41* (1986) 400.
9 G. Schneider, F. I. G. Landgraf and F. P. Missel, *J. Less-Common Met.*, *153* (1989) 169.